Smart Materials and Structures

PAPER • OPEN ACCESS

Auxetic 3D rotating octahedra frameworks

To cite this article: Mandy Leconte *et al* 2026 *Smart Mater. Struct.* **35** 015037

View the article online for updates and enhancements.

IOP Publishing Smart Mater. Struct. 35 (2026) 015037 https://doi.org/10.1088/1361-665X/ae3269

Smart Materials and Structures

RECEIVED
16 September 2025

REVISED
12 December 2025

ACCEPTED FOR PUBLICATION
31 December 2025

PUBLISHED
12 January 2026

PAPER

Auxetic 3D rotating octahedra frameworks

Mandy Leconte[1], Krzysztof K Dudek[2] and Luke Mizzi[1,*]

[1] Department of Sciences and Methods for Engineering, University of Modena and Reggio Emilia, Reggio Emilia, Italy
[2] Institute of Physics, University of Zielona Gora, ul. Szafrana 4a, Zielona Gora 65-069, Poland
[*] Author to whom any correspondence should be addressed.

E-mail: luke.mizzi@unimore.it

Keywords: auxetic metamaterials, hierarchical structures, rotating unit modes, lightweight systems

Abstract

Rotating unit metamaterials, as their name implies, are a class of auxetic systems which possess deformation mechanisms characterised by rotating blocks of material relative to one another. In this work, we propose a new class of hierarchical rotating unit systems made from octahedral frameworks connected to each other at the vertices. These systems, which are presented in terms of two distinct configurations: full-block and hierarchical ligament-based; were studied using a dual approach involving an extensive parametric finite element simulation run of various systems and experimental tests on prototype structures produced using stereolithography methods. These metamaterials have been shown to exhibit auxetic behaviour coupled with a high level of anisotropy, while other properties such as stiffness and volume fraction can also be tailored according to the necessary requirements. These properties make them ideal for potential applications in the fields of biomedical and aerospace engineering where lightweight systems with considerable stiffness and auxetic properties are often desirable.

1. Introduction

Mechanical metamaterials are systems with deformation behaviour that is defined by architecture rather than chemical composition. The design of metamaterials has attracted considerable interest over the past few decades, particularly due to their unique mechanical and physical properties which are not found in other materials. Auxetic metamaterials stand out for their negative Poisson's ratio [1–4], a characteristic that provides them with exceptional properties such as improved energy absorption [5, 6], increased indentation resistance [7] and enhanced acoustic properties [8–10]. This distinctive property opens applications in various fields, ranging from aerospace [11, 12], personal protection [13] and sports [14] to biomedical engineering [15, 16], where materials capable of controlled and reversible deformation are highly desirable. In recent years, the advent of additive manufacturing techniques has allowed for the realisability of many metamaterial architectures at the macro and microscale. As a result, research on mechanical metamaterials has advanced significantly since previously unrealisable architectures have become easier to produce.

Since auxeticity is a geometry-dependent property, it may be obtained at several scales ranging from the marco- [17, 18] to the micro- [19, 20] and nano/molecular level [21–27]. Many geometric configurations which give rise to auxetic behaviour have been developed, with the most important cases including re-entrant honeycomb models [28–30], chiral geometries [31–34], as well as rotating rigid or semi-rigid unit modes [35, 36]. In this work, we will focus on the latter class of structures. Rotating units are structures composed of blocks of material connected at their vertices which rotate relative to each other upon loading. Numerous examples of these 2D structures exist, such as the rotating square system [37, 38], as well as systems involving parallelograms [39–41], rhombi [40], triangles [42], mixed polygon models [43–45] and hierarchical structures [19, 46–49]. These systems can exhibit a wide range of Poisson's ratios from high positive values to giant negative ones as well as an extremely large spectrum of Young's moduli. These systems can also be extended to 3D structures, such as geometries containing cubes serving as the rigid units [50], perforated rotating unit modes [51] and modified hybrid geometries [52].

Despite these advancements, several challenges remain in the field of rotating auxetic metamaterials. One of these challenges involves the fact that while rotating units are typically considered to be the class of auxetic metamaterials with the highest level of structural stiffness, they are also characterised with a relatively large density and a low degree of strain tolerance and fatigue resistance. One method which has been employed in the literature to improve this factor is to introduce hierarchical truss elements within the system [53–58]. Provided that the correct geometric arrangement is chosen, the system can be designed in such a manner to retain its negative Poisson's ratio properties while simultaneously enhancing its stiffness/density ratio. This improvement is obtained through a change in deformation mechanism which involves the ligaments making up the rotating unit, hence reducing the localised stress concentrations at the interconnection regions of the system.

In this work, we aim to design lightweight 3D rotating unit auxetic metamaterials based on the same concept. Our focus will be on the rotating octahedron structure, which possess a representative unit cell made up of eight octahedra connected at the vertices which has the ability to exhibit a negative Poisson's ratio. This will be carried out using an integrated approach that combines numerical simulations with experimental testing on additively manufactured prototypes. The specific steps include designing two separate configurations of the 3D octahedron-based structure and conducting a parametric numerical study to analyse the influence of geometric variables on mechanical properties. The two configurations involve a full-block system and a hierarchical truss corresponding system. This will be followed by an experimental study involving 3D-printed systems subjected to uniaxial compressive loading tests.

2. Methodology

In order to investigate these systems, the finite element method (FEM) was used to conduct a parametric study and analyse the deformation behaviour of these metamaterials under uniaxial loading conditions. Following this step, an experimental and nonlinear numerical analysis was conducted on two selected configurations representative of the octahedral rotating unit metamaterial in order to validate the simulation results and observe the high strain behaviour of these systems.

The structures considered in this study are shown in figure 1. The representative volume element (RVE) of these 3D system consists of 8 octahedra joined together at the vertices. In the first case (see figure 1(a)) a full block structure was considered, where the rotating unit is a solid regular octahedron. This structure represents the classic 3D rotating unit mode; i.e. a system in which the 'rigidity' of the rotating unit is ensured through the use of a full-block of material. The second case (see figure 1(b)), on the other hand, involves a hierarchical truss geometry where the rotating unit is composed of beam-like ligaments. The trusses form the outer skeletal framework structure of the octahedron and are also joined together in the centre, in a manner analogous to a BCC cubic lattice. In both cases, the interconnection region is made up of a spherical connection which has the same radius as the cylindrical cross-section of the ligaments, at the edges of the octahedra.

As shown in figure 1, both these metamaterial architectures may be defined by the following geometric parameters: the side length of the octahedral rotating unit, l, the radius of the cross-section of the cylindrical ligaments/interconnection region, r, and the two angles θ and ϕ which define the rotational configuration of the octahedron. The angle θ defines the rotation in the xz-plane while ϕ is the rotation in the xy-plane. In this parametric study, the parameter l was kept constant at a value of 20 mm for all configurations studied, while the dimension r was set at 0.5 mm and 1 mm. The thicknesses were selected to account for both thin, long ligaments in the former case as well as thick ligaments in the latter. It is also worth noting, that in the case of the full-block systems, a small r value results in a system with thin overlapping interconnection regions, while a large r value results in a thicker connection between the vertices of the octahedra. Additionally, several different angular geometric configurations were considered for each of the two cases. These consisted of cases ranging from almost fully closed configurations (i.e. $\phi = 5°$, $\theta = 5°$) to *quasi*-fully opened forms (i.e. $\phi = 35°$, $\theta = 45°$). At this point, it is worth noting that the parameter ϕ was varied only between 5° and 35° since the 45° configuration represents the theoretical limit for the retention of connectivity of the same set of vertices and due to practical considerations related to the interconnection region geometry, configurations with ϕ values from 35° to 45° were not physically realisable as rotating unit systems. The full list of variables is indicated in table 1.

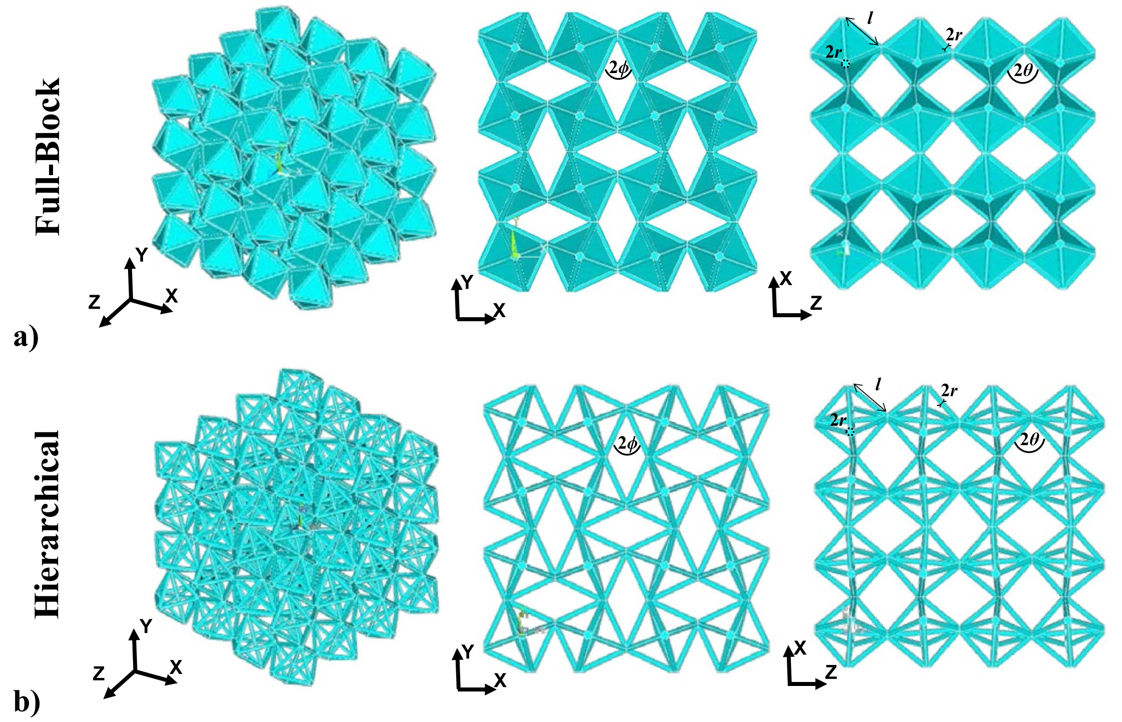

Figure 1. Images showing 2 × 2 × 2 supercells of the (a) full-block and (b) hierarchical rotating octahedra systems.

Table 1. List of geometric parameters used.

Geometric parameters	
l	20 mm
θ	5°–85° in steps of 5°
ϕ	5°–35° in steps of 5°
r	0.5 and 1 mm

The simulations were carried out using ANSYS Mechanical APDL software. Each system was simulated as 1/8th of a representative unit cell, i.e. a single octahedron, subjected to periodic boundary conditions (PBC) as shown in figure 2. This was possible since these systems possess three-axes of mirror-symmetry and thus this approach can be utilised to minimise computational time [59]. The systems were meshed using SOLID187 elements (a higher-order 3D 10-noded element with quadratic displacement behaviour). Following convergence tests, a minimum mesh size of $r/4$ was chosen for the truss configurations while for the solid block systems a non-uniform mesh with refinement at the interconnection region (minimum 12 elements) was utilised. The material properties of elastic photopolymerised resin were used with a Young's modulus of 1 MPa and a Poisson's ratio of 0.4 [60].

In order to obtain the mechanical properties of these structures, the systems were subjected to uniaxial compressive loading in the x, y and z-directions separately. As shown in figure 2, roller unidirectional displacement fixes were applied on the three faces located in the minimal positions in the x, y and z-directions. A uniaxial compressive displacement was applied at the surface orthogonal to the loading direction, while and the other maximal faces were constrained to always remain aligned with the principal Cartesian global axis directions throughout deformation using displacement coupling equations. From these simulations, the three on-axis effective Young's moduli and six Poisson's ratios were obtained.

In addition to the FEM simulations, two prototype systems (shown in figure 3) were fabricated using a FormLabs® Form 3 stereolithography 3D-printer in elastic resin. These two systems (one full-block and one hierarchical) were corresponding structures and each possessed the following set of parameters: $l = 20$ mm, $r = 1.0$ mm, $\theta = 40°$ and $\phi = 20°$. Each system was printed as a 2 × 2 × 2 supercell and subjected to uniaxial loading tests in the three principal directions. The Poisson's ratios were measured using digital image correlation methods over a strain range of *ca.* 6% compressive strain. The strain measurements were obtained by tracking the vertical and horizontal vertices of the lattice structures.

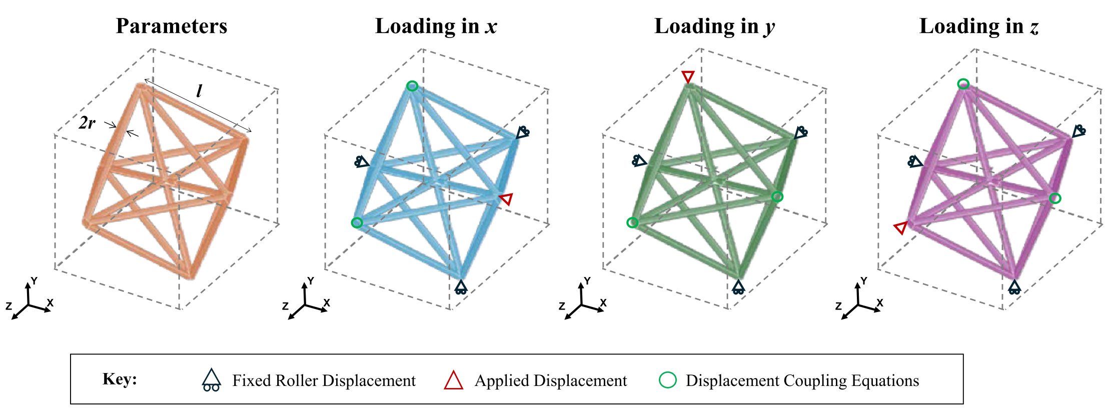

Figure 2. Images showing 1/8th of a RVE with the fixes and constraints used to load the systems in uniaxially in the x, y and z-directions, separately, under periodic boundary conditions.

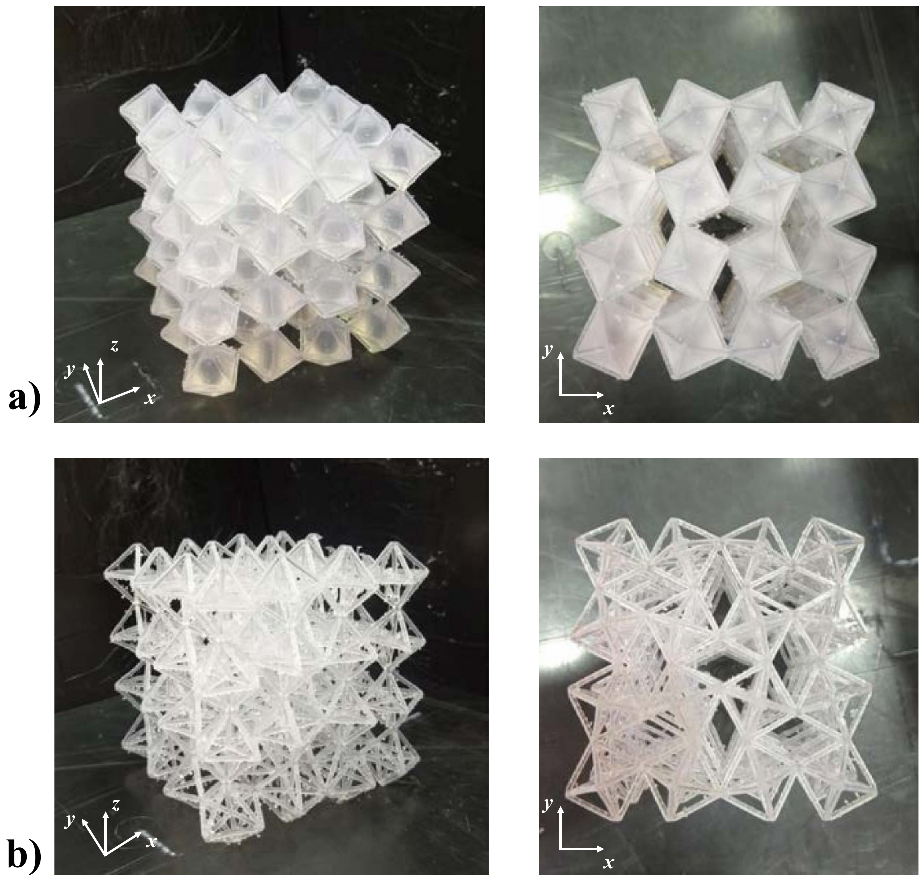

Figure 3. Images of the two 3D printed prototypes: (a) full-block and (b) hierarchical ligament systems.

3. Results and discussion

In this section, we present and discuss the results obtained from the parametric FEM analysis and the experimental tests performed on 3D-printed prototypes. The results of the finite element simulations, based on different geometric configurations for $r = 0.5$ and 1 mm, are first detailed. These results are then compared with the experimental data obtained from compression tests, allowing for an assessment of the consistency and validity of the numerical models.

3.1. Parametric FE simulations

It is clearly evident from the plots that these systems are highly anisotropic and all configurations exhibit a negative Poisson's ratio in at least two directions. The Poisson's ratio varies significantly, with values as low as −1.51 being observed in some planes while in other planes it is steadily close to zero. The lowest values were consistently observed for ν_{yx} and ν_{zx}, while the least negative values were obtained for ν_{yz} and ν_{zy}. It is also worth noting that all graphs exhibit a distinct symmetry with respect to the angle θ. This symmetry, which also exists with respect to the angle ϕ, indicates a regularity in the structural deformation when the angular configurations are varied. This observation indicates that the variation of the Poisson's ratio from $\theta = 5°$ to $\theta = 45°$ is identical to the variation from $\theta = 45°$ to $\theta = 85°$, reflecting the symmetry of the geometry of the octahedra used. Furthermore, as expected, the metamaterial configurations composed of filled octahedra possess a higher volume fraction and also a greater effective Young's modulus in comparison to configurations based solely on ligaments. The latter parameter is a dimensionless constant calculated by dividing the metamaterial system's Young's modulus with that of the constitutive material Young's modulus.

3.1.1. Thin ligament/interconnection region systems ($r = 0.5$ mm)

The plots in figure 4 show the variations of Poisson's ratios (ν_{xy}, ν_{xz}, ν_{yx}, ν_{yz}, ν_{zx}, ν_{zy}), along with graphs representing the volume fraction (V_{f}) and the effective Young's moduli (E^*_x, E^*_y, E^*_z) for the simulated systems with $r = 0.5$ mm. The results obtained clearly show that both the filled and ligament-based systems exhibit auxetic behaviour with similar trends observed for changes in the angles θ and ϕ.

It is evident that the solid octahedra-based systems show slightly more negative Poisson's ratio in comparison to the ligament-based systems. For the solid octahedra, the most negative Poisson's ratios were observed for the configuration with $\theta = 20°$ and $\phi = 30°$ for ν_{zx} at −1.41, while for the same system, a relatively large auxetic Poisson's ratio value of −1.11 was also observed for ν_{yx}. For the majority of other configurations, Poisson's ratios in the range of −1.0 and −0.6 were observed for ν_{zx} and ν_{yx}. On the other hand, for ν_{xy} and ν_{xz}, the Poisson's ratio varies significantly from −1.0 to 0 depending on the combination of θ and ϕ. For the former case, the most negative values were observed for systems with θ close to 45° and the least negative for $\theta = 5°$ and $\phi = 5°$ (or $\theta = 85°$ and $\phi = 5°$). This trend was completely reversed for ν_{xz}. Finally, for ν_{yz} and ν_{zy}, all configurations exhibiting a positive or *quasi*-zero Poisson's ratio. This suggests an insensitivity of these coefficients to the geometric configuration due to the mechanistic limitations imposed by the lack of rotation in the *zy*-plane. The distribution of positive values for ν_{yz} and ν_{zy} indicate that the deformation mechanism does not favour auxetic behaviour in this plane.

These trends were almost completely mirrored by the ligament-based systems, which exhibit almost identical behaviour in terms of Poisson's ratio. The greatest differences can be observed in the plots for the effective Young's modulus which show that the hierarchical ligament-based configurations possess a significantly reduced stiffness in comparison to the full-block corresponding structures. This was to be expected, as some deformation is absorbed by the ligaments, which have a reduced capacity to support loads without excessive deformation. It is also noted that in each case the highest stiffness was observed for configurations where θ equals 45° for E_z despite this configuration having the lowest relative volume fraction. This can be attributed to the fact that this configuration represents the fully opened form of the rotating octahedra mechanism, hence at this exact configuration the rotating mechanism is inhibited and as a consequence the system has a higher effective Young's modulus. However, this also results in a positive Poisson's ratio for this specific configuration since the mechanism responsible for imparting auxeticity cannot function effectively.

Figure 5 illustrates the undeformed and deformed forms for two representative full-block and ligament-based structures, providing a visual comparison of how these systems behave under compressive loading. It is evident that rotation of the octahedral unit is occurring in both configurations, however in the hierarchical system, this rotation is also accompanied by flexural deformation of the ligaments making up octahedron. This flexural deformation is almost uniformly distributed throughout the ligaments as a result of the stretch-dominated internal hierarchical structure of the ligament arrangement, in this case a square pyramidal framework [61]. In previous studies on lightweight hierarchical rotating unit auxetic systems [53, 54], it has been consistently shown that the selection of such triangular (in the case of 2D systems) and tetrahedron-based (in the case of 3D systems) frameworks results in uniform deformation (contraction or expansion) within the rotating unit which accompanies the overall rotation of the block and yields a resultant global negative Poisson's ratio. Therefore, during tensile loading, the flexure of the ligaments results in the octahedra stretching (whilst retaining their original relative dimensions) while rotating, thus retaining the auxeticity of the original rotating unit mode (see figure 5(b)).

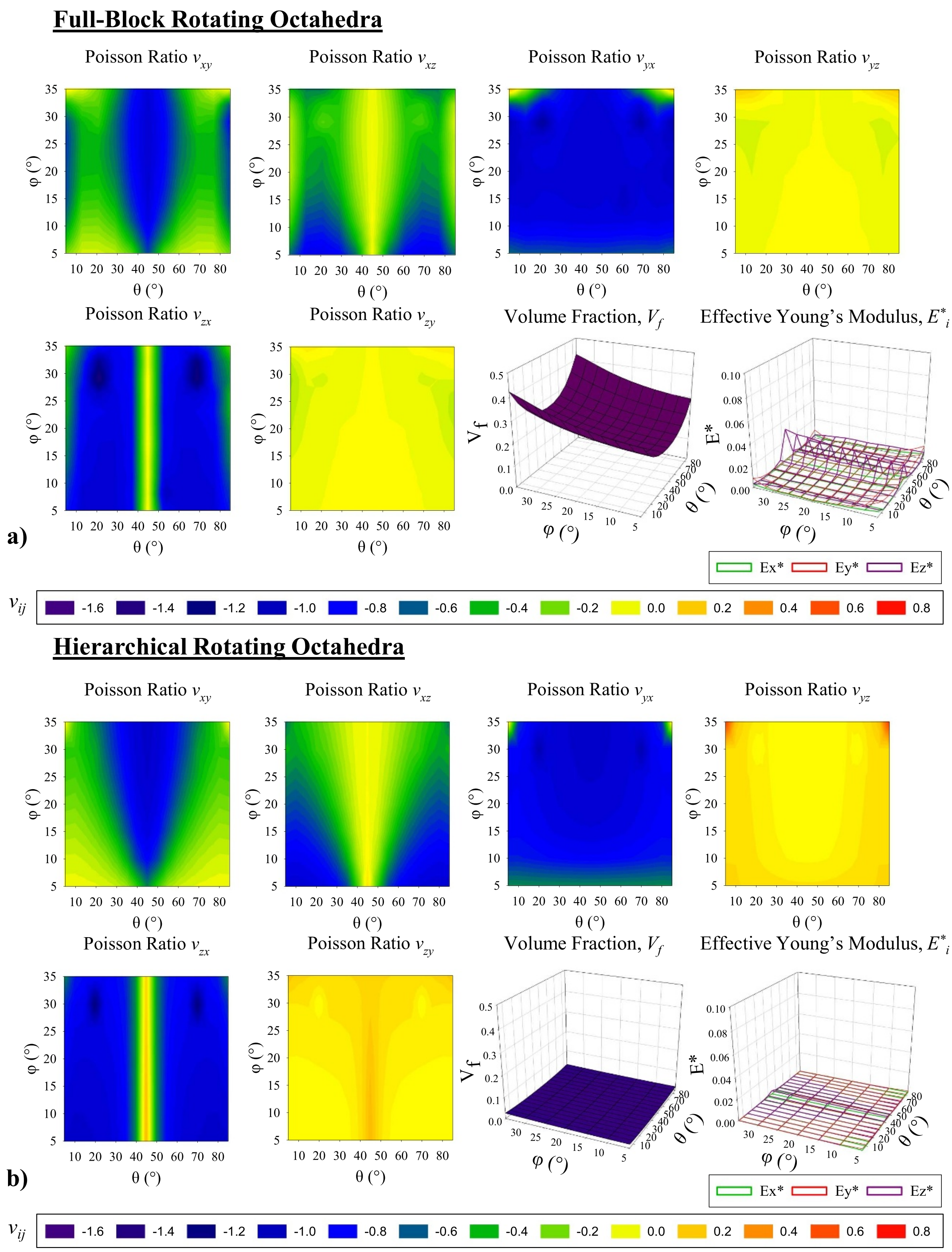

Figure 4. Plots showing how the Poisson's ratios, volume fraction and effective Young's moduli of the thin ligament/interconnection region ($r = 0.5$ mm) configurations varied with changing rotation angles θ and ϕ for (a) full-block and (b) hierarchical frameworks.

This effect indicates that the chosen hierarchical arrangement is sufficiently robust to retain the original auxeticity of the full-block rotating octahedra metamaterial.

The deformation of the ligaments in the hierarchical framework is also the main reason for the reduced overall Young's modulus of this configuration in comparison to the full-block system. However, the fact that the localised von Mises strains are distributed throughout the ligaments making up the rotating unit also means that the magnitude of these stresses is significantly lower, indicating that this configuration has a higher strain tolerance before fracture occurs. In the full-block system, all the localised strains are concentrated at the interconnection region, resulting in a maximum localised strain which is more than twice as high as that observed for the corresponding hierarchical system at the same global strain level (see figure 5). This factor is mainly responsible for the relatively low strain tolerance

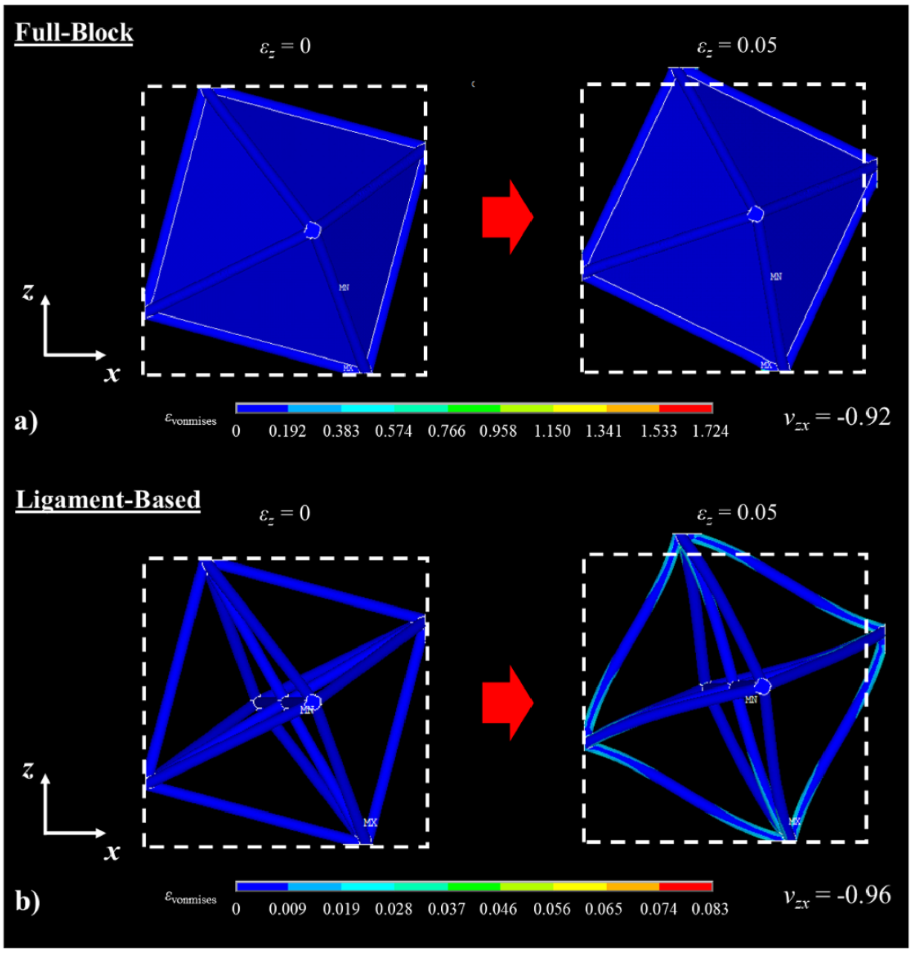

Figure 5. Deformations and localised von Mises strain distributions of two representative $r = 0.5$ mm structures in (a) the full-block configuration and (b) the hierarchical ligament-based configuration.

of 3D full-block rotating auxetic structures, which typically undergo small strain failure at the interconnection regions between rotating units.

3.1.2. Thick ligament/interconnection region systems ($r = 1.0$ mm)

As shown in figure 6, for the thick ligament/interconnection region configurations, the overall magnitude of Poisson's ratio was generally lower in comparison to the systems in the previous set with $r = 0.5$ mm. This was to be expected since by increasing the value of this parameter, the interconnection region between rotating units becomes thicker, leading to a reduced effectiveness of the rotating mechanism and increased stiffness. In fact, the latter point is clearly evident from the effective Young's modulus plots where it is shown that these systems have a significantly higher value in comparison to the previous set of structures.

The trends obtained for the Poisson's ratios are similar to the previous set; v_{xy} and v_{xz} continue to show the most auxetic behaviours, but with lower magnitudes compared to thin interconnection region systems, while the v_{yz} and v_{zy} coefficients remain mostly positive. It is also worth noting that the differences between hierarchical ligament-based and full-block rotating octahedra structures are less pronounced in terms of Poisson's ratio. This was also to be expected, since as the ligaments making up the octahedra get thicker, they become less amenable to flexure and hence the systems behave more similarly to the filled corresponding structures as shown in figure 7. However, in some singular, isolated cases, systems with $r = 1$ mm exhibited more negative Poisson's ratio than their $r = 0.5$ mm counterparts, such as the case of $\theta = 20°$ and $\phi = 30°$ for ν_{zx} which showed an extremely auxetic Poisson's ratio of -1.5. In the case of stiffness, it is clearly evident that these systems, as expected, show a higher overall effective Young's modulus. Similarly to the thin ligament systems, the highest stiffness is observed for loading in the z-direction, E_z, for systems with $\theta = 45°$, 5° and 85°. These configurations represent the full-opened and fully-closed configurations of the rotating octahedra.

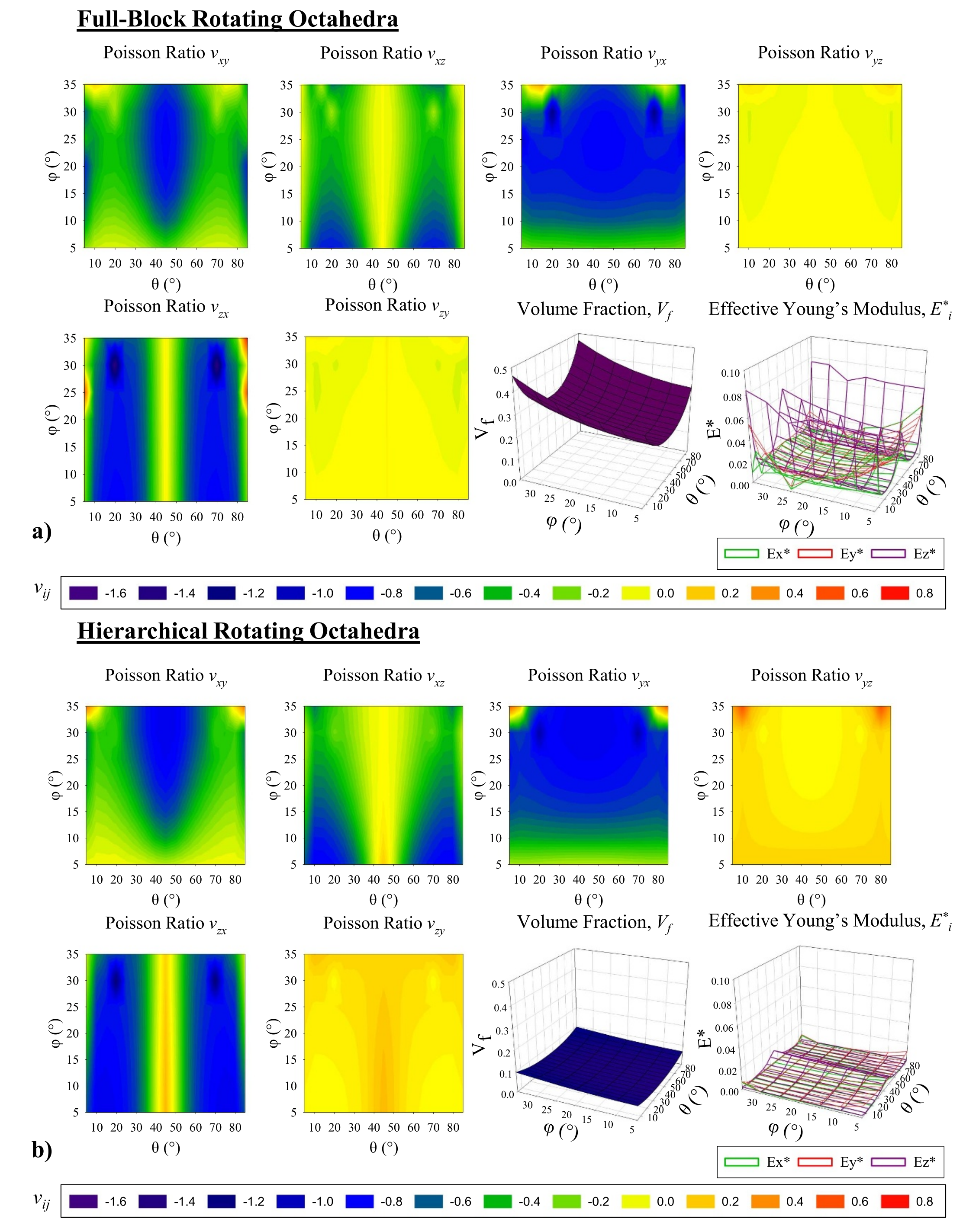

Figure 6. Plots showing how the Poisson's ratios, volume fraction and effective Young's moduli of the thick ligament/interconnection region ($r = 1.0$ mm) configurations varied with changing rotation angles θ and ϕ for (a) full-block and (b) hierarchical frameworks.

It is evident from figure 7, that the flexure of ligaments in the thick-ligamented hierarchical system is less pronounced than in the case of the thin-ligament system. This reduced flexural deformation, results in a similar von Mises localised strain value for both the full-block and hierarchical system and therefore, in this case, the introduction of hierarchy does not improve the strain tolerance of the metamaterial geometry.

3.1.3. Variable interconnection/ligament thickness, r

It is clear that the interconnection/ligament thickness, defined by the variable r, is a key factor which determines the mechanical properties and deformation behaviour of the rotating metamaterial systems. Therefore, in order to investigate more thoroughly the influence of this parameter on the mechanical

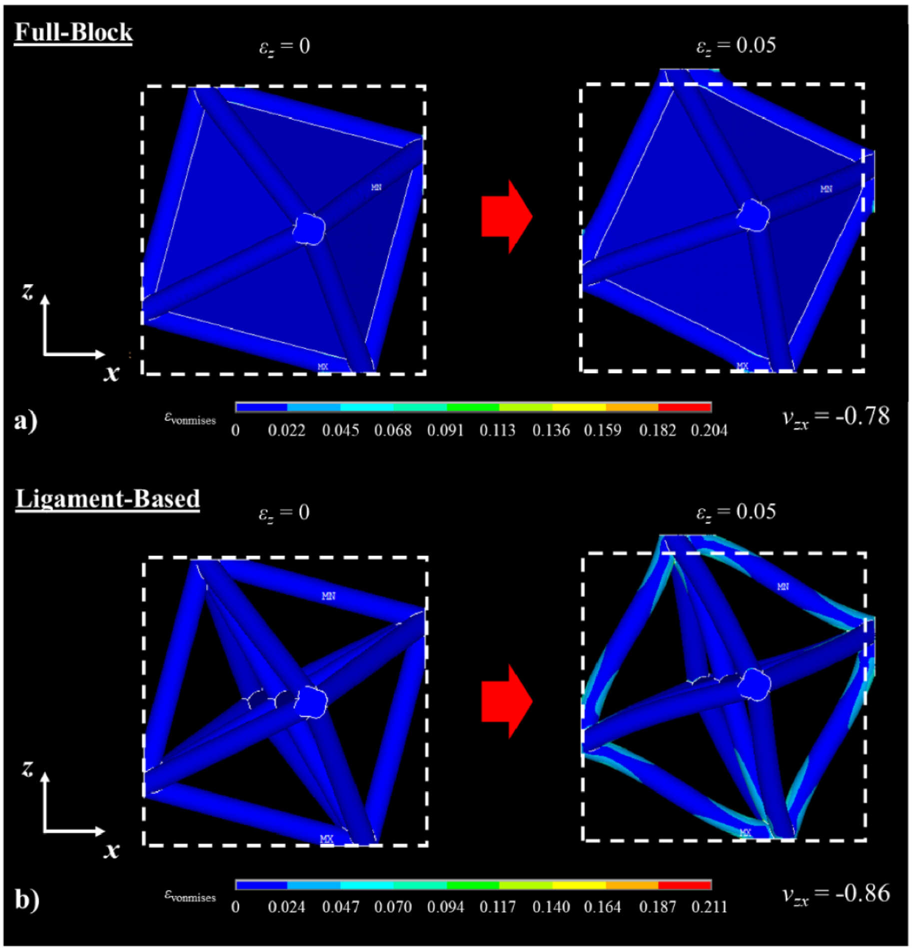

Figure 7. Deformations and localised von Mises strain distributions of two representative $r = 1.0$ mm structures in (a) the full-block configuration and (b) the hierarchical ligament-based configuration.

properties of these systems, an additional simulation run was carried out where this variable was varied while keeping the other geometric parameters constant, namely $\theta = 40°$, $\phi = 20°$, and $l = 20$ mm. The results obtained are presented in figure 8.

In terms of Poisson's ratio, it is immediately evident that both the full-block and hierarchical systems exhibit almost identical trends. In all cases, the most negative Poisson's ratio is observed for the systems with the smallest r value, i.e. $r = 0.5$ mm while the least auxetic systems are those with the highest thickness; $r = 2.5$ mm. For the Poisson's ratios v_{xy} and v_{xz}, which show the largest variation, the values vary from *ca.* -1 for the thinnest systems to -0.2 for the thickest systems. This change can be attributed to the interconnection region as systems with thick interconnection regions are less amenable to rotating deformations with respect to those with thinner connections. Nonetheless, it is interesting to note that the introduction of hierarchy appears to have a minimal effect on auxeticity. In previous studies on 3D hierarchical rotating cube systems [54], a noticeable reduction in the magnitude of the negative Poisson's ratio is observed once the full-block systems are compared with corresponding hierarchical systems, however this factor is not evident here. This change is probably due to the fact that rotating octahedra frameworks are connected together solely through vertices rather than through edges and vertices as in rotating cube systems which in the latter case results in a slight change of deformation mechanism once hierarchical configurations are introduced within the rotating unit. Vertex-based connections have a significantly lower stiffness in comparison to edge-based connections and therefore, a possible hypothesis which explains this behaviour could be that even with the introduction of hierarchy, which lowers the rigidity of the rotating octahedra significantly, 'hinge joint'-type rotations are still kinematically the favoured deformation mode. On the other hand, in rotating systems possessing edge-based connections between rotating units such as a rotating cubes, the high stiffness of these connections ensures that the role of other alternative deformation mechanisms such as localised flexure of ligaments plays a more significant role, thus altering the resultant Poisson's ratio of the metamaterial system.

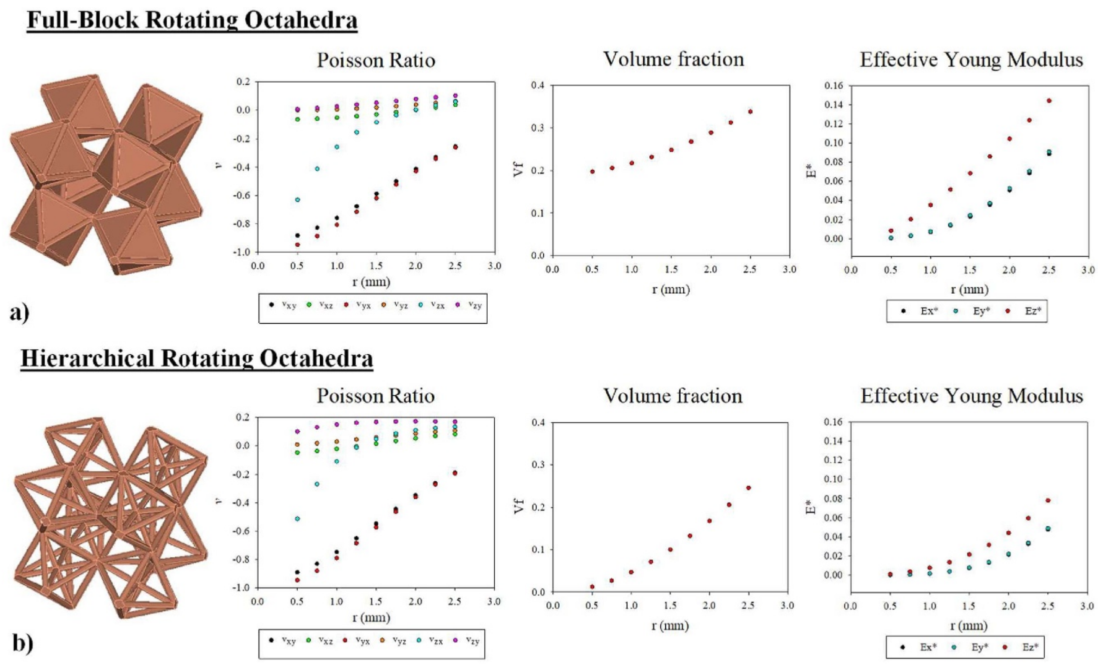

Figure 8. Deformations and localised von Mises strain distributions of two representative $r = 1.0$ mm structures in (a) the full-block configuration and (b) the hierarchical ligament-based configuration.

The results obtained for the effective Young's moduli are also of interest. While, as expected, the full-block systems exhibit a higher value than the hierarchical systems, the differences between the two systems are not extremely vast. At large r values, the full-block systems show stiffness values which are slightly more than double those observed for the hierarchical structures, with the differences being larger for corresponding systems with smaller r values. Despite the discrepancies in magnitude, the overall trends are identical for both sets of systems. In terms of volume fraction, it is also shown that the hierarchical systems have significantly reduced values with respect to the full-block systems. At $r = 0.5$ mm, the difference is at its maximum, with the hierarchical system being one order of magnitude lower, and hence lighter, than its corresponding full block system, while for the thickest systems; $r = 2.5$ mm, the ratio of V_f between hierarchical and full-block is closer to 70%.

3.2. Experimental results

In this section, the results pertaining to the experimental tests on the additively-manufactured prototypes are presented. As shown in figure 9, the systems were uniaxially loaded in the x-, y- and z-directions and the Poisson's ratios in the three principal planes were measured: ν_{xy}, ν_{xz}, ν_{yx}, ν_{yz}, ν_{zx}, ν_{zy}. In addition, nonlinear geometric simulations were carried out on these systems under PBC in order to allow for a comparison between numerical predictions and experimental findings.

The congruence between the results obtained from the experimental tests and FE simulations is distinctly clear from the plots in figure 9. This similarity is present despite the fact that the Poisson's ratio for the experimentally-tested prototypes was extracted from the unbounded edges of the system while the nonlinear FE simulations were carried out under PBC, and highlights the minute influence which edge effects have on the deformation mechanism of the rotating octahedra system.

With regards to the Poisson's ratio of these systems, as predicted by the initial parametric simulation run, there is little difference between the values obtained for the full-block and hierarchical systems. A constant Poisson's ratio of *ca.* -0.9 was obtained for both configurations for ν_{xy} and ν_{yx}. As one may observe from figure 9(a), (b), (d) and (e), from this projection, the system resembles a 2D rotating system; a metamaterial structure which is characterised by a Poisson's ratio of -1 which is retained over large strains; hence the large constant negative Poisson's ratio. On the other hand, the both systems exhibit Poisson's ratio of nearly zero for ν_{xz}, ν_{yz} and ν_{zy}. Finally, for the ν_{zx} plane, a distinctly nonlinear Poisson's ratio is observed over a 6% compressive strain range, with the Poisson's ratio departing from a value of *quasi*-zero at small strains and becoming more negative (*ca.* -0.65) at higher strains according to the FE simulations. This trend is also mirrored in the experimental results, albeit, reaching more negative Poisson's ratio at the same strain range.

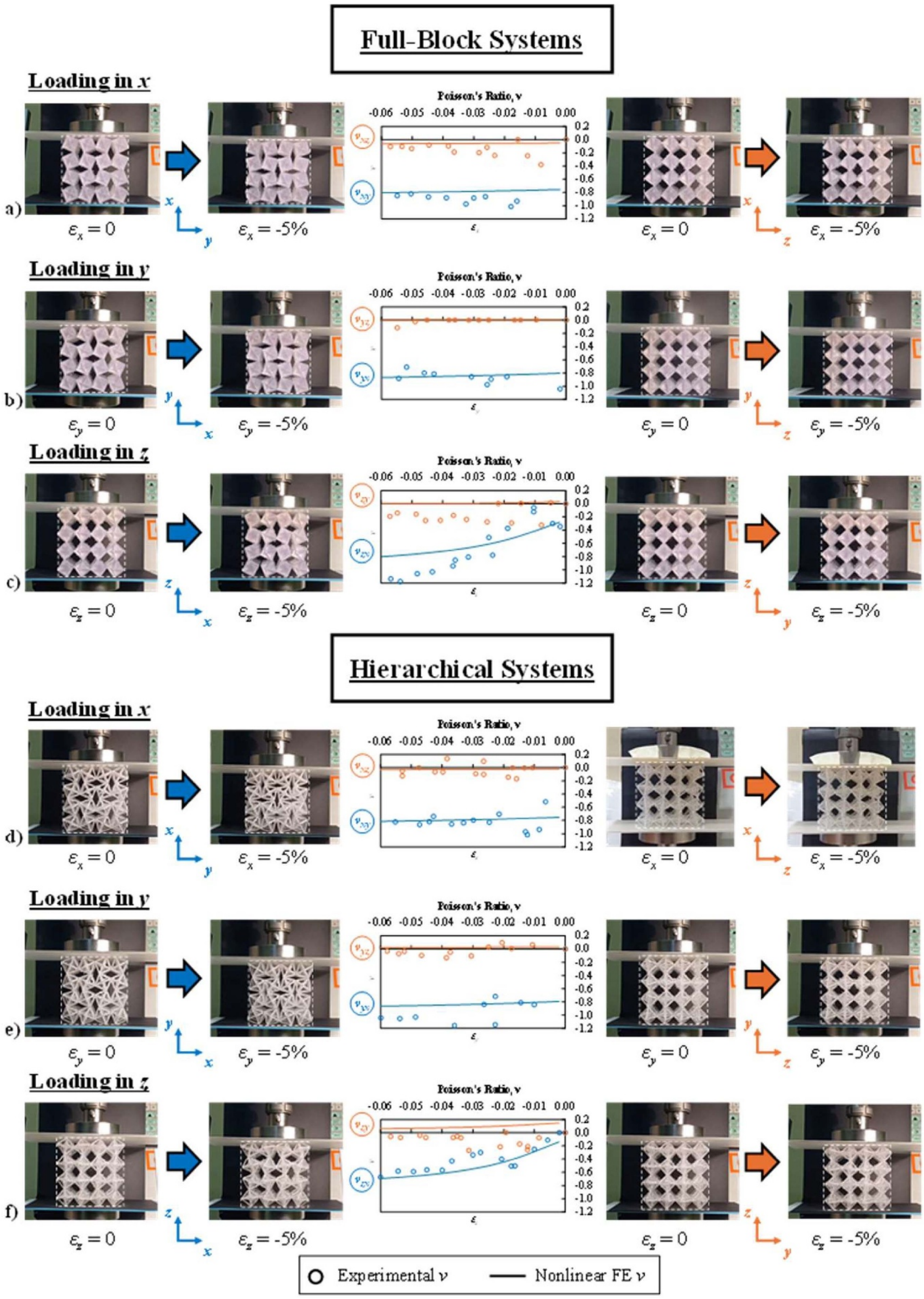

Figure 9. Plots and images showing the deformations and Poisson's ratios obtained for the full-block rotating octahedra (a)–(c) and hierarchical rotating octahedra (d)–(f) subjected to uniaxial loading in the *x*, *y* and *z*-directions. The circles represent the Poisson's ratios obtained from the experimental tests as extracted from the point-tracking analysis on the vertices of the system while the full lines are the predictions obtained from a geometric nonlinear FE analysis on systems with periodic boundary conditions.

Although we have only experimentally validated one set of geometric parameters, the extremely good match between experiments and simulation results for the mechanical properties and observed deformation mechanisms of these systems confirms the validity of the finite element simulation method used to simulate and analyse these structures. The latter results clearly highlight that there are some configurations with angular apertures θ and ϕ which are close to the limits of the rotating mechanism and thus, these configurations, which include systems with θ values close to 0°, 45° or 90° and a ϕ values close to 0° and 45°, are ideally to be avoided in order to ensure that the system functions as predicted.

Another point worth highlighting is the fatigue performance of these systems. All six loading tests; two in each direction to measure the six Poisson's ratios; were carried out on the same two prototypes. Both systems underwent all loading tests without breaking, however, the full-block systems showed reduced recovery and fractured in various points upon further loading despite its constituent material being a hyperelastic resin which can tolerate over 100% strain before breaking. On the other hand, the hierarchical ligament-based structure exhibited extremely high strain tolerance and even after repetitive loading at higher strains than those presented in figure 9 did not undergo failure. This observation confirms the results obtained from the analysis of localised von Mises strains which indicate that introduction of hierarchical ligament frameworks in these systems results in improved strain tolerance. The experimental prototypes tested in this work may be considered as systems analogous to the ones presented in figure 5, which have a similar l/r ratio of 20:1, and indicate that the maximum localised strain value in the ligamented system is about half that of its full-block counterpart.

3.3. General remarks

The systems presented in this work represent a new class of 3D auxetic metamaterials based on rotating octahedra with mechanical properties which may be tailored to obtain systems with a desired set of Poisson's ratios, Young's moduli and volume fraction. The Poisson's ratio may be customised primarily as a function of the geometric parameters l, r, θ and ϕ, while in the case of Young's moduli and volume fraction the use of full-block or hierarchical configurations is the greatest determining factor. In cases where high stiffness is required, full-block configurations are optimal, however if higher strain tolerances or lower weight are necessary, then hierarchical systems are the more appropriate option. This change in stiffness and density can be obtained without significant changes to the Poisson's ratio. These observations are consistent with findings in the literature on other 2D and 3D rotating unit systems which have been transformed into ligament-based hierarchical metamaterial structures. The combination of lightweightedness with relatively high stiffness and small strain cyclic deformation tolerance is a very desirable characteristic in prosthetic implants and aerospace components and it is envisaged that further studies on these lattice systems will focus primarily on the utilisation of geometric topological optimisation methods to obtain the ideal set of parameters for a fixed set of requirements. Further studies can also be carried out to form modified frameworks based on these systems which address certain structural weakpoints such as the interconnection regions in full-block configurations as well as the use of elongated octahedra to obtain more highly anisotropic configuration with a wider range of mechanical properties. Finally, the hierarchical framework utilised in this work can also be potentially applied to other 3D auxetic metamaterial systems in order to impart greater versatility and improved mechanical properties.

4. Conclusion

In this work, rotating octahedra-based auxetic metamaterials are proposed, numerically analysed and experimentally tested. Two configurations are produced: a full-block system and a hierarchical ligament-based framework. These systems were first analysed through an extensive parametric FE simulation run followed by experimental tests on additively-manufactured prototypes. The Poisson's ratios obtained from the two methods showed extremely good agreement and clearly demonstrate that these systems are characterised by high level of anisotropy along with the capacity to exhibit a wide range of negative Poisson's ratios. Furthermore, it was shown, that the level of auxeticity remains relatively unaffected by type of geometric configuration utilised (i.e. whether a full-block or hierarchical system is used), while the Young's moduli and volume fraction of the system vary significantly. This means that one may obtain a desired Poisson's ratio on the basis of the nominal geometric parameters while stiffness and weight may be controlled independently based on which framework is used to construct the octahedral rotating unit. This work demonstrates the high versatility of this class of auxetic systems and presents a route towards the design of lightweight 3D auxetic metamaterial systems.

Data availability statement

All data that support the findings of this study are included within the article (and any supplementary files).

Acknowledgment

This work was supported by the Fondazione Cariplo and Fondazione CDP Grant No. 2023-2526 'Support for Young Italian Researchers in ERC Competitions' awarded to Luke Mizzi. Krzysztof Dudek also acknowledges the support of the program of the Polish Ministry of Science under the title 'Regional Excellence Initiative', project no. RID/SP/0050/2024/1.

Author contributions

Mandy Leconte
Formal analysis (lead), Investigation (lead), Methodology (equal), Software (equal), Writing – original draft (lead)

Krzysztof K Dudek 0000-0002-9570-6713
Investigation (supporting), Methodology (supporting), Resources (supporting), Writing – review & editing (supporting)

Luke Mizzi 0000-0002-7650-1173
Conceptualization (lead), Formal analysis (supporting), Funding acquisition (lead), Investigation (supporting), Methodology (equal), Supervision (lead), Writing – review & editing (lead)

References

[1] Evans K E and Alderson A 2000 Auxetic materials: functional materials and structures from lateral thinking! *Adv. Mater.* **12** 617
[2] Bertoldi K, Vitelli V, Christensen J and Van Hecke M 2017 Flexible mechanical metamaterials *Nat. Rev. Mater.* **2** 17066
[3] Lakes R S 1987 Foam structures with a negative poisson's ratio *Science* **235** 1038–40
[4] Lakes R and Wojciechowski K W 2008 Negative compressibility, negative Poisson's ratio, and stability *Phys. Status Solidi b* **245** 545–51
[5] Jiang L and Hu H 2017 Low-velocity impact response of multilayer orthogonal structural composite with auxetic effect *Compos. Struct.* **169** 62–68
[6] Yuan S, Chua C K and Zhou K 2019 3D-PrintedMechanical metamaterials with high energy absorption *Adv. Mater. Technol.* **4** 1800419
[7] Duncan O, Chester M, Wang W, Alderson A and Allen T 2023 Effect of twist on indentation resistance *Mater. Today Commun.* **35** 105616
[8] He J H and Huang H H 2018 Tunable acoustic wave propagation through planar auxetic metamaterial *J. Mech.* **34** 113–22
[9] Dudek K K, Iglesias Martinez J A, Ulliac G, Hirsinger L, Wang L, Laude V and Kadic M 2023 Micro-scale mechanical metamaterial with a controllable transition in the poisson's ratio and band gap formation *Adv. Mater.* **35** 2210993
[10] Ruzzene M and Scarpa F 2005 Directional and band-gap behavior of periodic auxetic lattices *Phys. Status Solidi b* **242** 665–80
[11] Guo Y, Zhang J, Chen L, Du B, Liu H, Chen L, Li W and Liu Y 2020 Deformation behaviors and energy absorption of auxetic lattice cylindrical structures under axial crushing load *Aerosp. Sci. Technol.* **98** 105662
[12] Bettini P, Airoldi A, Sala G, Di Landro L, Ruzzene M and Spadoni A 2010 Composite chiral structures for morphing airfoils: numerical analyses and development of a manufacturing process *Composites B* **41** 133–47
[13] Li T, Liu F and Wang L 2020 Enhancing indentation and impact resistance in auxetic composite materials *Composites B* **198** 108229
[14] Duncan O, Shepherd T, Moroney C, Foster L, Venkatraman P D, Winwood K, Allen T and Alderson A 2018 Review of auxetic materials for sports applications: expanding options in comfort and protection *Appl. Sci.* **8** 941
[15] Zadpoor A A 2020 Meta-biomaterials *Biomater. Sci.* **8** 18–38
[16] Ali M N, Busfield J J and Rehman I U 2014 Auxetic oesophageal stents: structure and mechanical properties *J. Mater. Sci., Mater. Med.* **25** 527–53
[17] Mizzi L, Hoseini S F, Formighieri M and Spaggiari A 2023 Development and prototyping of SMA-metamaterial biaxial composite actuators *Smart Mater. Struct.* **32** 035027
[18] Cicala G, Recca G, Oliveri L, Perikleous Y, Scarpa F, Lira C, Lorato A, Grube D J and Ziegmann G 2012 Hexachiral truss-core with twisted hemp yarns: out-of-plane shear properties *Compos. Struct.* **94** 3556–62
[19] Dudek K K, Martínez J A I, Ulliac G and Kadic M 2022 Micro-scale auxetic hierarchical mechanical metamaterials for shape morphing *Adv. Mater.* **34** 2110115
[20] Mizzi L, Salvati E, Spaggiari A, Tan J C and Korsunsky A M 2020 2D auxetic metamaterials with tuneable micro-/nanoscale apertures *Appl. Mater. Today* **20** 100780
[21] Tretiakov K V 2009 Negative Poisson's ratio of two-dimensional hard cyclic tetramers *J. Non Cryst. Solids* **355** 1435–8
[22] Wojciechowski K W 2003 Non-chiral, molecular model of negative Poisson ratio in two dimensions *J. Phys. A: Math. Gen.* **36** 11765–78
[23] Wojciechowski K and Branka A 1989 Negative Poisson ratio in a two-dimensional "'isotropic"' solid *Phys. Rev. A* **40** 7222–5
[24] Narojczyk J W, Tretiakov K V, Smardzewski J and Wojciechowski K W 2023 Hardening of fcc hard-sphere crystals by introducing nanochannels: auxetic aspects *Phys. Rev. E* **108** 045003

[25] Tretiakov K V, Pigłowski P M and Wojciechowski K W 2023 Auxeticity modifications and unit cell doubling in Yukawa fcc crystals with [001]-nanochannels filled by hard spheres *Smart Mater. Struct.* **32** 025008
[26] Tretiakov K V and Wojciechowski K W 2020 Auxetic, partially auxetic, and nonauxetic behaviour in 2D crystals of hard cyclic tetramers *Phys. Status Solidi Rapid Res. Lett.* **14** 2000198
[27] Suzuki Y, Cardone G, Restrepo D, Zavattieri P D, Baker T S and Tezcan F A 2016 Self-assembly of coherently dynamic, auxetic, two-dimensional protein crystals *Nature* **533** 369–73
[28] Masters I G and Evans K E 1996 Models for the elastic deformation of honeycombs *Compos. Struct.* **35** 403–22
[29] Yang L, Harrysson O, West H and Cormier D 2015 Mechanical properties of 3D re-entrant honeycomb auxetic structures realized via additive manufacturing *Int. J. Solid Struct.* **69–70** 475–90
[30] Evans K E, Alderson A and Christian F R 1995 Auxetic two-dimensional polymer networks an example of tailoring geometry for specific mechanical properties *J. Chem. Soc. Faraday Trans.* **91** 2671–80
[31] Alderson A, Alderson K L, Attard D, Evans K E, Gatt R, Grima J N, Miller W, Ravirala N, Smith C W and Zied K 2010 Elastic constants of 3-, 4- and 6-connected chiral and anti-chiral honeycombs subject to uniaxial in-plane loading *Compos. Sci. Technol.* **70** 1042–8
[32] Gatt R, Attard D, Farrugia P-S, Azzopardi K M, Mizzi L, Brincat J-P and Grima J N 2013 A realistic generic model for anti-tetrachiral systems *Phys. Status Solidi b* **250** 2012–9
[33] Mizzi L and Spaggiari A 2021 Chiralisation of Euclidean polygonal tessellations for the design of new auxetic metamaterials *Mech. Mater.* **153** 103698
[34] Wojciechowski K W 1989 Two-dimensional isotropic system with a negative poisson's ratio *Phys. Lett. A* **137** 60–64
[35] Grima-Cornish J N, Attard D, Grima J N and Evans K E 2021 Auxetic behavior and other negative thermomechanical properties from rotating rigid units *Phys. Status Solidi Rapid Res. Lett.* **16** 2100322
[36] Saxena K K, Das R and Calius E P 2016 Three decades of auxetics research — materials with negative poisson's ratio: a review *Adv. Eng. Mater.* **18** 1847–70
[37] Grima J N and Evans K E 2000 Auxetic behavior from rotating squares *J. Mater. Sci. Lett.* **19** 1563–5
[38] Ishibashi Y and Iwata M 2000 A microscopic model of a negative poisson's ratio in some crystals *J. Phys. Soc. Japan* **69** 2702–3
[39] Attard D, Manicaro E and Grima J N 2009 On rotating rigid parallelograms and their potential for exhibiting auxetic behaviour *Phys. Status Solidi b* **246** 2033–44
[40] Grima J N, Farrugia P S, Gatt R and Attard D 2008 On the auxetic properties of rotating rhombi and parallelograms: a preliminary investigation *Phys. Status Solidi b* **245** 521–9
[41] Mizzi L, Attard D, Evans K E, Gatt R and Grima J N 2021 Auxetic mechanical metamaterials with diamond and elliptically shaped perforations *Acta Mech.* **232** 779–91
[42] Grima J N and Evans K E 2006 Auxetic behavior from rotating triangles *J. Mater. Sci.* **41** 3193–6
[43] Lim T C 2022 An auxetic metamaterial based on rotating and nonrotating rigid units inspired by an aztec geometric pattern *Phys. Status Solidi b* **259** 2200385
[44] Lim T C 2024 auxetic system based on rotating hexagons and triangles *Phys. Status Solidi b* **261** 2300586
[45] Lim T C 2024 Auxetic metamaterial model made from rotating rectangles, hexagons, and triangles *Phys. Status Solidi b* **261** 2400343
[46] Li X, Fan R, Fan Z and Lu Y 2021 Programmable mechanical metamaterials based on hierarchical rotating structures *Int. J. Solid Struct.* **216** 145–55
[47] Gatt R, Mizzi L, Azzopardi J I, Azzopardi K M, Attard D, Casha A, Briffa J and Grima J N 2015 Hierarchical auxetic mechanical metamaterials *Sci. Rep.* **5** 8395
[48] Tang Y, Lin G, Han L, Qiu S, Yang S and Yin J 2015 Design of hierarchically cut hinges for highly stretchable and reconfigurable metamaterials with enhanced strength *Adv. Mater.* **27** 7181–90
[49] Cho Y *et al* 2014 Engineering the shape and structure of materials by fractal cut *Proc. Natl Acad. Sci. USA* **111** 17390–5
[50] Attard D and Grima J N 2012 A three-dimensional rotating rigid units network exhibiting negative poisson's ratios *Phys. Status Solidi b* **249** 1330–8
[51] Galea R, Farrugia P S, Dudek K K, Attard D, Grima J N and Gatt R 2023 A novel design method to produce 3D auxetic metamaterials with continuous pores exemplified through 3D rotating auxetic systems *Mater. Des.* **226** 111596
[52] Gao Y, Wei X, Han X, Zhou Z and Xiong J 2021 Novel 3D auxetic lattice structures developed based on the rotating rigid mechanism *Int. J. Solid Struct.* **233** 111232
[53] Mizzi L and Spaggiari A 2020 Lightweight mechanical metamaterials designed using hierarchical truss elements *Smart Mater. Struct.* **29** 105036
[54] Mizzi L, Dudek K K, Frasinetti A, Spaggiari A, Ulliac G and Kadic M 2025 Lightweight 3D hierarchical metamaterial microlattices *Adv. Sci.* **12** 2410293
[55] Meza L R, Zelhofer A J, Clarke N, Mateos A J, Kochmann D M and Greer J R 2015 Resilient 3D hierarchical architected metamaterials *Proc. Natl Acad. Sci. USA* **112** 11502–7
[56] Rayneau-Kirkhope D 2018 Stiff auxetics: hierarchy as a route to stiff, strong lattice based auxetic meta-materials *Sci. Rep.* **8** 12437
[57] Han D, Ren X, Zhang Y, Yu Zhang X, Gang Zhang X, Luo C and Min Xie Y 2022 Lightweight auxetic metamaterials: design and characteristic study *Compos. Struct.* **293** 115706
[58] Hao J, *et al* 2022 Novel dual-platform lightweight metamaterials with auxeticity *Eng. Struct.* **270** 114891
[59] Mizzi L, Attard D, Gatt R, Dudek K K, Ellul B and Grima J N 2021 Implementation of periodic boundary conditions for loading of mechanical metamaterials and other complex geometric microstructures using finite element analysis *Eng. Comput.* **37** 1765–79
[60] Elastic 50A resin datasheet. nd (available at: https://formlabs-media.formlabs.com/datasheets/2001420-TDS-ENUS-0.pdf)
[61] Ashby M F 2005 The properties of foams and lattices *Proc. R. Soc. A* **364** 15–30